HAL
open science

Diagnostic interest of whole-body MRI in early- and late-onset LAMA2 muscular dystrophies: a large international cohort

Susana Quijano-Roy, Jana Haberlova, Claudia Castiglioni, John Vissing, Francina Munell, Francois Rivier, Tanya Stojkovic, Edoardo Malfatti, Marta Gómez García de La Banda, Giorgio Tasca, et al.

To cite this version:

Susana Quijano-Roy, Jana Haberlova, Claudia Castiglioni, John Vissing, Francina Munell, et al.. Diagnostic interest of whole-body MRI in early- and late-onset LAMA2 muscular dystrophies: a large international cohort. Journal of Neurology, 2022, 269, pp.2414-2429. 10.1007/s00415-021-10806-0 . hal-03359688

HAL Id: hal-03359688

https://hal.science/hal-03359688

Submitted on 30 Sep 2021

HAL is a multi-disciplinary open access archive for the deposit and dissemination of scientific research documents, whether they are published or not. The documents may come from teaching and research institutions in France or abroad, or from public or private research centers.

L'archive ouverte pluridisciplinaire **HAL**, est destinée au dépôt et à la diffusion de documents scientifiques de niveau recherche, publiés ou non, émanant des établissements d'enseignement et de recherche français ou étrangers, des laboratoires publics ou privés.

Diagnostic interest of whole-body MRI in early- and late-onset *LAMA2* muscular dystrophies: a large international cohort

Susana Quijano-Roy[1,2] · Jana Haberlova[3] · Claudia Castiglioni[4,5] · John Vissing[6] · Francina Munell[7] · François Rivier[8,9] · Tanya Stojkovic[10] · Edoardo Malfatti[11] · Marta Gómez García de la Banda[1] · Giorgio Tasca[12] · Laura Costa Comellas[7] · Audrey Benezit[1] · Helge Amthor[1,2] · Ivana Dabaj[1,13] · Clara Gontijo Camelo[14] · Pascal Laforêt[15] · John Rendu[16] · Norma B. Romero[17,18] · Eliana Cavassa[1] · Fabiana Fattori[19] · Christophe Beroud[20] · Jana Zídková[21] · Nicolas Leboucq[22] · Nicoline Løkken[6] · Ángel Sanchez-Montañez[23] · Ximena Ortega[24] · Martin Kynčl[25] · Corinne Metay[26,27] · David Gómez-Andrés[7] · Robert Y. Carlier[28]

Abstract

Background LAMA2-related muscular dystrophy (LAMA2-RD) encompasses a group of recessive muscular dystrophies caused by mutations in the *LAMA2* gene, which codes for the alpha-2 chain of laminin-211 (merosin). Diagnosis is straightforward in the classic congenital presentation with no ambulation and complete merosin deficiency in muscle biopsy, but is far more difficult in milder ambulant individuals with partial merosin deficiency.

Objective To investigate the diagnostic utility of muscle imaging in LAMA2-RD using whole-body magnetic resonance imaging (WBMRI).

Results 27 patients (2–62 years, 21–80% with acquisition of walking ability and 6 never ambulant) were included in an international collaborative study. All carried two pathogenic mutations, mostly private missense changes. An intronic variant (c.909 + 7A > G) was identified in all the Chilean cases. Three patients (two ambulant) showed intellectual disability, epilepsy, and brain structural abnormalities. WBMRI T1w sequences or T2 fat-saturated images (Dixon) revealed abnormal muscle fat replacement predominantly in subscapularis, lumbar paraspinals, gluteus minimus and medius, posterior thigh (adductor magnus, biceps femoris, hamstrings) and soleus. This involvement pattern was consistent for both ambulant and non-ambulant patients. The degree of replacement was predominantly correlated to the disease duration, rather than to the onset or the clinical severity. A "COL6-like sandwich sign" was observed in several muscles in ambulant adults, but different involvement of subscapularis, gluteus minimus, and medius changes allowed distinguishing LAMA2-RD from collagenopathies. The thigh muscles seem to be the best ones to assess disease progression.

Conclusion WBMRI in LAMA2-RD shows a homogeneous pattern of brain and muscle imaging, representing a supportive diagnostic tool.

Keywords Merosin · Congenital muscular dystrophy · Heatmap · Muscle MRI · Myopathy

Abbreviations

IHC	Immunohistochemical
MDC1A	Merosin-deficient congenital muscular dystrophy type 1A
LGMD-R23	Limb girdle muscular dystrophy R23
LHBF	Long head of biceps femoris
WBMRI	Whole-body magnetic resonance imaging

✉ David Gómez-Andrés
david_gomez@vhebron.net

Introduction

LAMA2-related muscular dystrophy (LAMA2-RD) constitutes one of the most frequent forms of congenital muscular dystrophy. It is the result of the lack of functional laminin-α2 chain, which is part of the heterotrimeric laminin-211 (also known as merosin), a secreted protein present at the basement membrane that participates in sarcolemmal attachment to muscle cells. This protein is coded by the *LAMA2* gene (6q22-23), which contains 65 exons [1].

Clinical manifestations of LAMA2-RD range between two extreme phenotypes: the earliest and most severe form,

a congenital muscular dystrophy characterized by congenital hypotonia and severe weakness (MDC1A) and the mildest form, a limb-girdle muscular dystrophy presenting with proximal weakness in childhood or even adulthood (LGMD-R23) [2–4]. As observed in other genetic muscle disorders, intermediate phenotypes also exist. The severity spectrum is closely related to immunohistochemical and genetic features. Severe phenotypes show a profound depletion or absence of merosin expression in muscle or skin (complete merosin deficiency) and tend to carry null mutations [3, 6]. Clinically, while patients with complete deficiency are unable to reach unsupported walking, those with residual expression show milder phenotypes and may stand or walk. In these cases, molecular analysis often reveals missense mutations [2, 7]. In addition, the incorporation of next-generation sequencing techniques to clinical practice has led to the emergence of atypical phenotypes, in particular individuals with predominant central nervous system involvement and subtle muscle manifestations [5].

At the diagnostic level, severe LAMA2-RD is an easily recognizable disease with straightforward results in the diagnostic tests (increased CK levels, brain white matter changes, dystrophic features, and merosin deficiency in the muscle biopsy). In contrast, milder cases with later onset or less defined features may be more challenging to diagnose. Isolated motor delay or proximal weakness in an intelligent child with increased CK levels is quite unspecific and the interest in performing a brain MRI may be unclear even for expert clinicians. Moreover, detecting the partial deficiency on muscle may be difficult, often requiring several antibodies, due to the large size of the protein. Furthermore, molecular diagnosis may remain elusive, despite next-generation sequencing techniques, in particular, due to the frequent occurrence of large intragenic deletions and duplications (up to 20% of cases) or intronic mutations [7].

In this context, the use of muscle imaging may have an additional interest. Recognizable patterns of muscle involvement have been described in different early-onset myopathies [8–10]. However, there is scarce data published on LAMA2-RD muscle imaging, limited mostly to the lower limbs, where it has shown an overlap with Bethlem myopathy [11]. Identifying a whole-body muscle MRI pattern (WBMRI) in this disease would facilitate diagnosis in several situations: (1) atypical phenotypes (e.g. mental retardation in an ambulant patient) [5]; (2) clinical overlap with other myopathies associating joint contractures (collagenopathies, laminopathies) [12]; (3) myopathies associated with increased CK levels [3]; (4) inconclusive *LAMA2* genetic results (variants of unknown significance or elusive second mutation) [3]; (5) pediatric or adult patients with muscle weakness and myopathic unspecific features on muscle biopsy [13]. Moreover, it seems urgent to gain insight into the disease evolution and accelerates the development of imaging biomarkers, in view of the extraordinary therapeutic achievements occurring in the field [14–16].

Here, through a large collaborative international study, we collected WBMRI examinations from a broad spectrum of LAMA2-RD patients with different ages and severities. The aims were to explore the muscle signal changes, to investigate the homogeneity of patterns in early and late-onset entities (MDC1A and LGMD-R23), and identify those muscles best correlated with disease progression.

Methods

Ethics statement

All evaluations were performed in the setting of "standard of care", and all the retrospective data analyzed were maintained completely anonymous.

Patients

We evaluated 27 patients (18 females and 9 males) from 23 months to 62 years of age. Most patients were Caucasians from European countries, but non-Caucasian patients with familiar origins from other continents were also represented: South America (Chile 4), North Africa (Algeria 1, Morocco, 3), and Asia (India 1).

Six patients had a more severe congenital form and never walked unsupported (non-ambulant group). Twenty-one patients achieved independent ambulation and showed proximal weakness (ambulant group). All patients carried two pathogenic mutations in *LAMA2* gene.

If available, we collected information regarding muscle biopsy. Specifically, we collected the global morphological pattern (dystrophic vs. myopathic) and immunolabelling of C-terminal laminin-α2 chain (80 kDa) and of the N-terminal laminin α2 chain (300 kDa).

Genetic analysis, bioinformatics analysis, and variant interpretation

The pathogenicity of variants was determined according to current ACMG guidelines [17]. Variants were filtered out according to their allele frequency ($\leq 1\%$) as reported in the GnomAD database (http://gnomad.broadinstitute.org/). Each variant was then evaluated considering a review of the literature, the location of the variant in the gene and the

Table 1 Clinical features of patients

Patients who never reached independent ambulation

Patient code	Age	Gender	Origin (country)	LAMA2 mutations	Age of onset	Muscle biopsy (300 kD, 80 kD antibodies)	Maximal motor function	Actual motor function	Ventilation support	Cognitive impairment	Seizures	Brain MRI	Muscle MRI technique
F1	23 m	F	Morocco	c.8244 + 1G > A Homozygous	2 weeks	Dystrophic,300—/80 NA	Sitting	Sitting	No	No	No	WM changes	T1/STIR WBMRI
F2	27 m	F	Europe (Spain)	c.1467 + 1G > C, c.3038-7G > A	2 months	Dystrophic, 300—/ 80 NA	Sitting	Sitting	No	No	No	WM changes	T1/STIR WBMRI
F3	7y	F	Algeria	c.1377delC Homozygous	5 months	Dystrophic, 300-/80-	Sitting	Sitting	Yes, nocturnal BiPaP	No	No	WM changes	DIXON WBMRI IDEAL
F4	7y	M	Asia (India)	c.1823_1824delAT, Homozygous	Birth	Dystrophic, 300 NA/80 NA	Standing with support	Sitting	No	Learning disability	No	WM changes	DIXON WBMRI IDEAL
F5	19y	F	Europe (France)	del exons 9 -34, del exons 23–34	Birth	Dystrophic, 300—/80-	Sitting	Sitting	Yes, BiPaP	Mental retardation	Yes	WM changes + occipital increased cortical thickness	T1/STIR WBMRI
F6	20y	F	Europe (Spain)	c.5116C > T, c.7074C > A,	1 month	Dystrophic, 300—/80 NA	Sitting	Sitting	Yes, nocturnal BiPAP	No	No	WM changes	T1/STIR WBMRI

Patients who reached independent ambulation

Patient code	Age	Gender	Origin (country)	LAMA2 mutations	Age of onset	Muscle biopsy (300 kD, 80 kD antibodies)	Maximal motor function	Actual motor function	Ventilation support	Cognitive impairment	Seizures	Brain MRI	Muscle MRI technique
P1	3y	F	European (Poland)	c.2049–2050 c.2166A > T	Birth	Dystrophic, 300 NA/80 NA	Walking	Walking with support	No	No	No	WM changes	T1/STIR WBMRI
P2	8y	F	European (France)	c.1793_1795 del c.3294delG	1y	Not available	Walking	Walking	No	Learning difficulties	No	WM changes	T1/STIR WBMRI
P3	8y	F	European (France)	c1798_1800 delGGA c.5116C > T	1.5y	Dystrophic, 300 NA/80 NA	Walking	Walking	No	No	No	WM changes	T1/STIR WBMRI
P4	8y	F	European (France)	c.3718C > T c.6706A > G	Birth	Not available	Walking	Walking	No	No	No	Not brain MRI but brain observed in muscle MRI	T1/STIR WBMRI
P5	13y	M	European (Czech Rep)	c.799G > A, c.3691G > T	3 years	Not available	Walking	Walking	No	No	No	WM changes	T1/STIR WBMRI
P6	15y	M	South America (Chile)	c. (909 + 7A > G), c.[1467 + 2 T > C]	1 y	Dystrophic, 300 NA/80 NA	Walking	Walking	No	Learning dificulties	No	WM changes	T1/STIR WBMRI

Table 1 (continued)

Patients who reached independent ambulation													
Patient code	Age	Gender	Origin (country)	LAMA2 mutations	Age of onset	Muscle biopsy (300 kD, 80 kD antibodies)	Maximal motor function	Actual motor function	Ventilation support	Cognitive impairment	Seizures	Brain MRI	Muscle MRI technique
P7	16y	M	European (Italy)	c.752 T > C Homozygous	1 Y	Dystrophic, 300 NA/80 NA	Walking	Walking	No	Mental retardation	Yes	WM changes, perisylvian and parieto-occipital polimicrogyria	T1/STIR WBMRI
P8	17y	F	European (Czech Rep)	c.611C > A, c.5235-18G > A	2 years	Dystrophic, 300 + /80 NA	Walking	Walking	No	No	No	WM changes	T1/STIR lower limb MRI + head MRI
P9	21y	M	South America (Chile)	c.[909 + 7A > G], c.[1854_1861dupACGTGTTC]	1 y	Dystrophic, 300 + /80 NA	Walking	Walking	No	No	No	WM changes	T1/STIR WBMRI
P10	26y	F	European (Italy)	c.7898 + 1G > T c.9257G > A	1,5 y	Dystrophic, 300 + /80 -	Walking	Walking	No	No	No	WM changes	Lower limb MRI
P11	28y	M	South America (Chile)	c. (909 + 7A > G) Homozygous	0.5y	Dystrophic, 300 NA/80 NA	Walking	Walking with support	Nocturnal BiPaP	No	No	WM changes	DIXON WBMRI IDEAL
P12	29y	F	Morocco	c.2230C > T Homozigous	Birth	Dystrophic, 300—/80 +	Walking	Walking	No	Learning difficulties	Yes	WM changes, perisylvian polimicrogyria and severe, posterior cortical dysplasia	T1/STIR WBMRI
P13	33y	F	European (France)	c.3038_7GA, c.8244 + 1G > A	Birth	Dystrophic, 300 NA/80 NA	Walking	Walking	No	No	No	WM changes	T1/STIR WBMRI
P14	36y	F	South America (Chile)	c.(909 + 7A > G) Homozygous	Birth	Dystrophic, 300 NA/80 NA	Walking	Wheel chair bound	Nocturnal BiPaP	Learning difficulties	No	WM changes	DIXON WBMRI IDEAL
P15	37y	F	European (Denmark)	c.35 T > G c.3758 T > G	0.7y	Dystrophic, 300 + /80 -	Walking	Walking	No	Speech delay	No	WM changes	T1/STIR WBMRI
P16	41y	F	European (France)	c.2749 + 1G > A c.4311 + 1G > A	5y	Dystrophic 300—/80 +	Walking	Walking	NA	No	No	NA	Lower limb MRI
P17	46y	F	European (France)	c.1793_1795del, c.6706A > G	27 y	Dystrophic, 300 + / 80 -	Walking	Walking	No	No	No	WM changes	DIXON WBMRI IDEAL
P18	61y	M	European (Denmark)	c.443G > A, c.397-13_398del	1 y	Dystrophic, 300 + / 80 -	Walknig	Walking	No	No	No	WM changes	T1/STIR WBMRI
P19	62y	M	European (Czech Rep)	c.799G > A, c.9095dupA	5y	Myopathic, 300 + / 80 NA	Walking	Walking with support	No	No	Yes	WM changes	T1/STIR WBMRI

Table 1 (continued)

Patients who reached independent ambulation													
Patient code	Age	Gender	Origin (country)	LAMA2 mutations	Age of onset	Muscle biopsy (300 kD, 80 kD antibodies)	Maximal motor function	Actual motor function	Ventilation support	Cognitive impairment	Seizures	Brain MRI	Muscle MRI technique
P20	42y	M	Morocco	c.7057 C > T Homozygous	22 y	Dystrophic, 300 NA/ 80 NA	Walking	Walking	No	No	No	WM changes	DIXON WBMRI IDEAL
P21	48y	F	European (France)	c.1791_1793del Homozygous	2 Y	Myopathic 300 + / 80 NA	Walking	Walking	Nocturnal BiPaP	Memory loss	No	WM changes	DIXON WBMRI IDEAL

Positive immunolabeling is indicated by "+" and absence or decreased immunolabeling, by −. Abbreviations: *F* female, *m* months, *M* male, *NA* not available, *y* years, *WM* white matter

resulting corresponding protein, in silico prediction tools and functional studies when available (details on supplemental Table 1). All considered variants have been confirmed by a second independent method.

MRI and systematic scoring

Twenty-four patients were examined using WBMRI techniques, following previously described protocols [8, 9, 18, 19]. The WBMRI examinations consisted of axial sequences from head to toes with T1 and STIR (17 patients) or Dixon T2 with fat and water images (7 patients). Three additional patients had segmental MRI examinations scanning only the lower limbs in two cases and the lower limbs and the head region in one case. T1-weighted sequences (fast spin-echo T1 or fat images of the T2 Dixon technique) were obtained to detect fat replacement of the muscle. T2 with fat saturation sequences (STIR or Water images of the T2 Dixon technique) were performed to search for white matter abnormalities in the brain and to explore the presence of edema or inflammation in the muscles. A senior radiologist and an experienced neurologist blinded to the patient's clinical and genetic data evaluated all T1 and T2 fat-saturated weighted images, including and assessed 109 muscles in each patient (54 muscle pairs and tongue). The degree of fatty replacement of muscle in T1 or fat images of the T2 Dixon was scored according to the abnormal signal intensity (1 normal muscle, 2 mild fatty replacement, 3 severe replacement and 4 extreme replacement or absence of muscular tissue) [20]. Considering the lack of asymmetries we observed in the disease, the median of left and right scores was used for the following analysis. Due to the extreme differences in ages, scoring of muscle bulk abnormalities was not considered.

Statistics

To analyze and represent the distribution of signal abnormalities in every muscle from each patient, we built heatmaps following previously published methods [21]. We used the regional heatmap to delineate the muscle "fingerprint" and hierarchical heatmaps to investigate the existence of patterns of fat replacement by clusters of muscles in different types of patients. Partial Spearman's rho correlation was used as an indicator of how the replacement in one particular muscle was related to disease duration (controlling by disease onset), or to disease onset (controlling by disease duration). Due to the exploratory nature of this analysis, we did not correct for multiple comparisons and restricted the study to ambulant patients. For those muscles in which scores were the most correlated with disease duration, we represented the cumulative probability of fatty replacement score along disease duration.

Results

Clinical features

To facilitate the description, we split the sample into two groups depending on the acquisition of walking ability. Their clinical, histological, and genetic data are summarized in Table 1. Most non-ambulant patients were children (median age: 7 years range 5 months–19.9 years) and presented at birth or in the first months of life, with hypotonia, motor delay, and high CK levels. In contrast, ambulant patients were examined usually at the adult age (median age: 26.7 years; range 23 months–62 years) and although onset was often during infancy, it varied from birth to 27 years. Hypotonia, motor delay, and abnormal walking or running were the most frequent initial symptoms.

Motor, respiratory and orthopedic complications were closely correlated in both groups. All patients in the non-ambulant group remained able to sit at the age of MRI study. The majority had developed a spinal deformity (4/6) and half of them received respiratory support. Ambulant patients were still able to walk except for three patients who required partial assistance and one who became wheelchair-bound. Two of these patients developed scoliosis and started nocturnal ventilation after puberty.

Although most patients showed normal cognitive function, 6 (5 in the ambulant group) patients had learning disabilities or speech delay, and two cases have intellectual disability. Epileptic seizures were only reported in three patients, being refractory in the two with intellectual disability.

Biopsy findings

A muscle biopsy was available in 23 patients. Non-ambulant cases (5) always showed dystrophic features. Immunohistochemical (IHC) studies revealed absent expression of merosin in all five biopsies. In the ambulant group, 16 out of the 18 biopsies showed dystrophic features, and the remaining two showed unspecific myopathic features. IHC studies were available in ten cases. Six of them were studied using both antibodies and a reduction was detected in all at least with one antibody, either 300 kDa or 80 KDa fragments. Of the four cases only studied by one antibody (300 kDa fragment), two did not reveal merosin deficiency compared to controls.

Genetic results

The genetic results are included in Table 1, Fig. 1 and supplemental Table 1, in which they are linked to previous publications [1, 7, 12, 22–26]. A total of 35 variants were identified. Among them, three mutations (c.4311 + 1G > A, c.2166A > T, and c.9257G > A) have not been reported so far in Clinvar, LOVD, and HGMD Pro databases and four had not been previously published (c.443G > A, c.6706A > G, c.1467 + 1G > C and c.1467 + 2 T > C). In terms of genetic variants, there were ten missense changes (29%), nine splicing changes (26%), and seven small deletions (20%). Other types of variants were less frequent, including five nonsense changes (14%) and two small duplications (5.5%). Two large deletions were found in one patient (5.5%). Among the 27 patients, 10 carry variants at the homozygous state. We confirmed that the variants were inherited from both parents, except for case 18 in which one of the parents' DNA was not available. This spectrum of mutations can be correlated to the *LAMA2* mutation database https://databases.lovd.nl/shared/genes/LAMA2, which reports 2035 public variants; among them, 344 represent unique public pathogenic variants related to disease, with a majority of substitutions (59%) and deletions (27%). Duplications (9%) are less described than in the reported study. In terms of their foreseeable impact, most of the variants in our cohort are either pathogenic truncating or splicing mutations (65%), fitting with the high level of truncating variants notified in the *LAMA2* database (74%).

Brain imaging findings

In all the cases in which head was explored by STIR, T2 fat-saturated sequences or Dixon (water-only-images), we found different degrees of white matter abnormalities that always spared corpus callosum, capsula interna, and cerebellum. All non-ambulant patients and a part of those having acquired walking showed diffuse and striking white matter changes. The remaining ambulant patients showed less diffuse abnormalities or even only patchy or very subtle changes (Fig. 2). White matter involvement was detectable either in STIR or T2 weighted images but due to poorer resolution, subtle involvement was less visible on STIR. In addition, abnormal cortical brain development was revealed in 3 patients, one non-ambulant and two ambulant patients. All these 3 cases showed epilepsy and cognitive impairment (two with intellectual disability and one with learning disability).

Regional heatmap: the LAMA2-RD "fingerprint"

WBMRI showed a homogeneous topography of the signal changes obtained by T1-weighted sequences or Dixon (fat-only images) throughout the series. There were not significant differences between the patterns observed in ambulant and non-ambulant patients. Figure 3 shows the regional heatmap of the global series, obtained after scoring fatty replacement, muscle by muscle, systematically ordered by

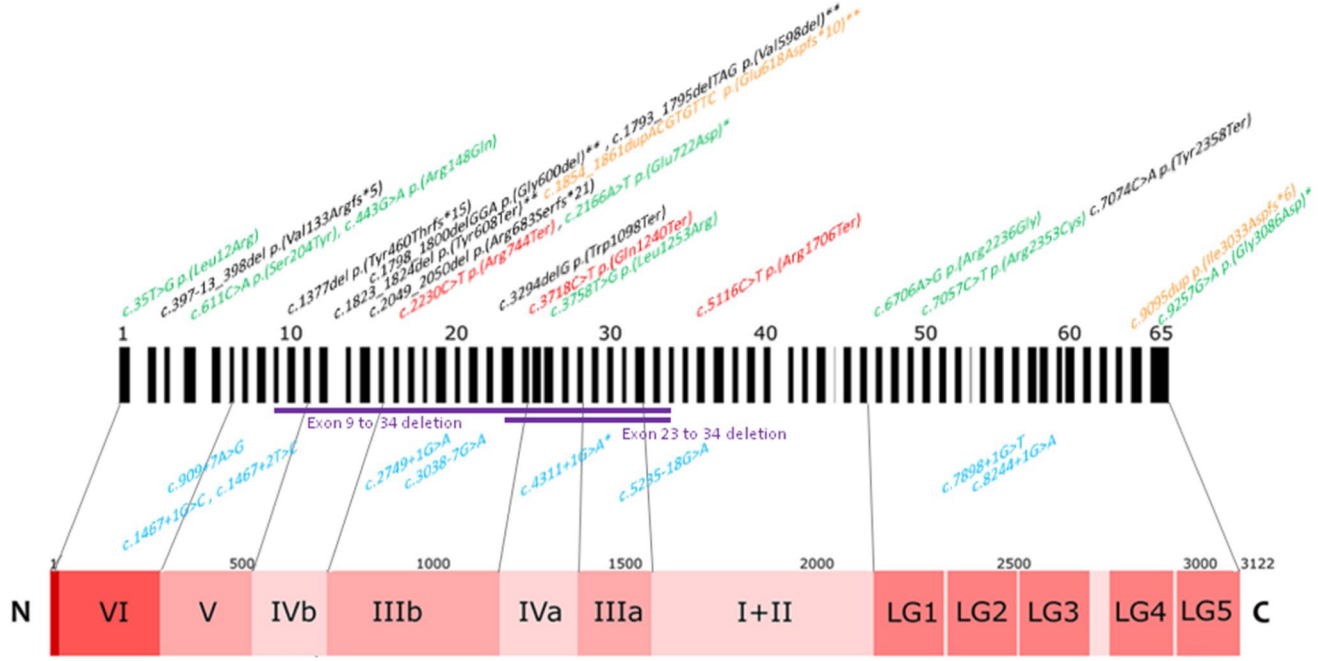

Fig. 1 LAMA2 variants in the cohort: Localization of the *LAMA2* variants of the reported patients. (*): never reported variant, (**): variants localized in exon 13. Splicing variants are colored in blue, missense in green, nonsense in red, small deletion in black and small duplication in orange. Laminin-alpha2 protein domains: I to VI, and Laminin G-like (LG) are shown in light pink to red boxes, from the C-terminal (C) to N-terminal region (N) (adapted from Oliveira et al. Hum Mut 2018)

regions of the body, as in previous reports for other myopathies [21, 27, 28]. Involvement in the head muscles preferably occurs in temporalis, while other muscles are relatively preserved at late stages. In the neck, extensor muscles are predominantly affected. In the scapular girdle, subscapularis muscle (Fig. 4, thick vertical white arrows) and serratus anterior are strikingly affected among surrounding muscles. The arm and the forearm are relatively spared in comparison to other regions. Axial muscles (erector spinae) are frequently abnormal, predominantly at the lumbar region. In the pelvis, gluteus medius and minimus are the most severely affected muscles (Fig. 4, thick horizontal white arrows). In contrast, gluteus maximus and psoas muscles are normal until advanced stages. In the thigh, the anterior compartment tends to be less affected than other compartments and shows a homogeneous involvement (similar degree of abnormality in vasti and rectus femoris muscles). In the medial compartment, adductor magnus often shows the most abnormal signal in the thigh, while adductor longus and brevis are more spared. In the posterior compartment, long head of biceps femoris (LHBF) and to a lesser degree, hamstrings (semimembranosus, semitendinosus) are predominantly affected (Fig. 4, black arrows). In contrast, the short head of biceps femoris, gracilis and sartorius muscles remain preserved. Leg muscles are affected after other regions (trunk, pelvis, thigh) with predominance of the posterior and lateral compartments. Soleus is the first muscle to be abnormal (Figs. 3 and 4), followed by gastrocnemii and peroneal muscles.

Global hierarchical heatmap: key muscles in LAMA2-RD

This method is used to identify groups of key muscles that allow recognizing the disease at different stages of muscle replacement. Seven "clusters" of muscles are delineated according to the degree of fat replacement (Fig. 5-A). Muscles from cluster 7 are those to be considered in early stages of the disease because they are consistently the most affected, showing marked replacement even in less affected patients ("positive fingerprint"). At the opposite end of the spectrum, muscles of cluster 1 are those that render diagnostic help at advanced stages of the disease, because they are preserved even when global muscle replacement is severe ("negative fingerprint"). In between these two major clusters, intermediate subsets of muscles are delineated. Clusters 2, 3 and 4 are constituted by muscles that are relatively spared in moderate or severe patients. Groups 5 and 6 account for muscles relatively affected in patients with mild or moderate global replacement. These latter groups are less useful in diagnosis but may constitute key muscles in the follow-up of the disease.

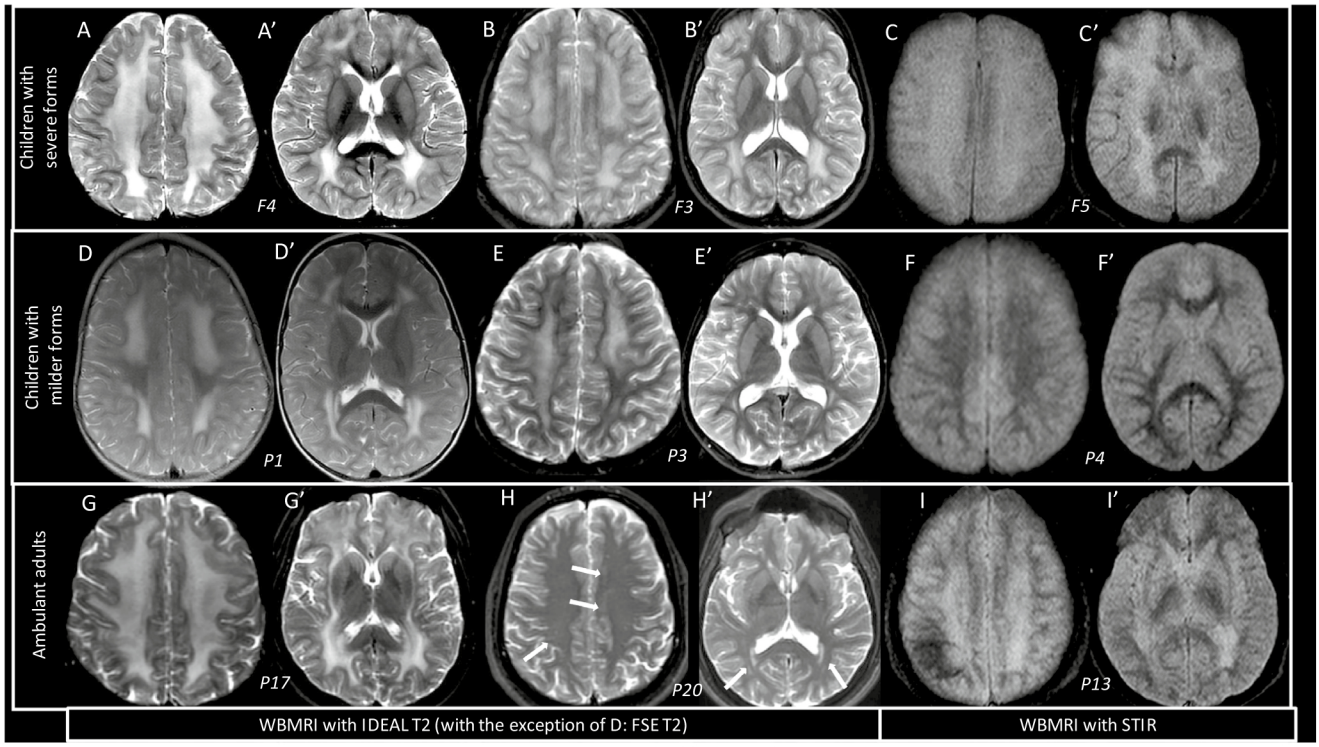

Fig. 2 Brain MRI images in non-ambulant children **A–C** ambulant children **D–F**, and ambulant adults **F–I**. Selection of two axial slices for nine patients (A to I) located on centrum semiovale and foramina of Monroe (') with the same neuro-ocular reference planes. A, B and C are brain images from children presenting a severe myopathy and who never acquired walking ability. All patients show severe and diffuse changes in the white matter sparing corpus callosum and capsula interna. D, E and F are brain images from children with milder forms, who were able to walk. In D and E white matter changes are diffuse; in contrast, in F they are very subtle. G, H and I are adult ambulant patients. White matter changes are diffuse in G and I and subtle in H (arrows). All the slices are part of the whole-body MRI examinations except for the patient D. For this patient the slices have been acquired during a dedicated brain MRI. For A, B, E, G and H, the images are water images of the IDEAL T2 (DIXON type) of the brain acquired during the WB MRI with the head coil. For C, F and I the images are STIR images of the brain acquired during the WB MRI with the head coil. White matter involvement is detectable either in STIR or T2-weighted images but resolution and subtle involvement is less visible on STIR. This technical point has convinced us to prefer IDEAL T2 WB MRI examination in young child to have a sufficient brain analysis

No relevant differences were found in the pattern of muscle fatty replacement when comparing ambulant and non-ambulant patients (Fig. 5-B). Non-ambulant patients showed minimal abnormalities at a very early stage of the disease but they presented severe signal changes at earlier ages than ambulant patients.

Relationship of muscle fatty replacement with disease duration and onset

To study the relationship between replacement scores and disease duration or age of onset, we used the partial Spearman's rho correlation coefficient in the ambulant group. In most involved muscles, signal changes are closely related to the disease duration (Figs. 3 and 6-A). Several muscles seem to have a better relationship between replacement scores and disease duration, particularly in the thigh: tensor fasciae latae (partial rho = 0.872, CI 95% 0.675–0.949), LHBF (partial rho = 0.849, CI 95% 0.621–0.939), semitendinosus (partial rho = 0.838, CI 95% 0.672–0.942), rectus femoris (partial rho = 0.837, CI 95% 0.595–0.922) and latissimus dorsi (partial rho = 0.778, CI 95% 0.492–0.926) (Fig. 6-B).

Other results

Abnormal striated banding collagen VI-like "sandwich sign" within several muscles (vastus lateralis, rectus anterior, triceps—Fig. 4U, deltoid, soleus—Fig. 4R) was identified in adult ambulant patients with a Bethlem-like phenotype [8, 29]. None of the patients showed clear abnormalities in the STIR sequences or the water-only Dixon images.

Discussion

This international study describes the muscle imaging features together with molecular, clinical, and histological characteristics of LAMA2-RD patients with a wide

Fig. 3 Regional heatmap representing scores for T1 signal in ambulant and non-ambulant patients with LAMA2-related dystrophy. The dendrogram above the heatmap represents the similarities between patients (the closer the junction to the bottom is, the more similar two patients are). Muscles are ordered according to different body regions. Shading represents the intensity of muscle changes (see legend in the left upper part of the figure). Disease duration, severity phenotype, and motor status when MRI was performed are shown below

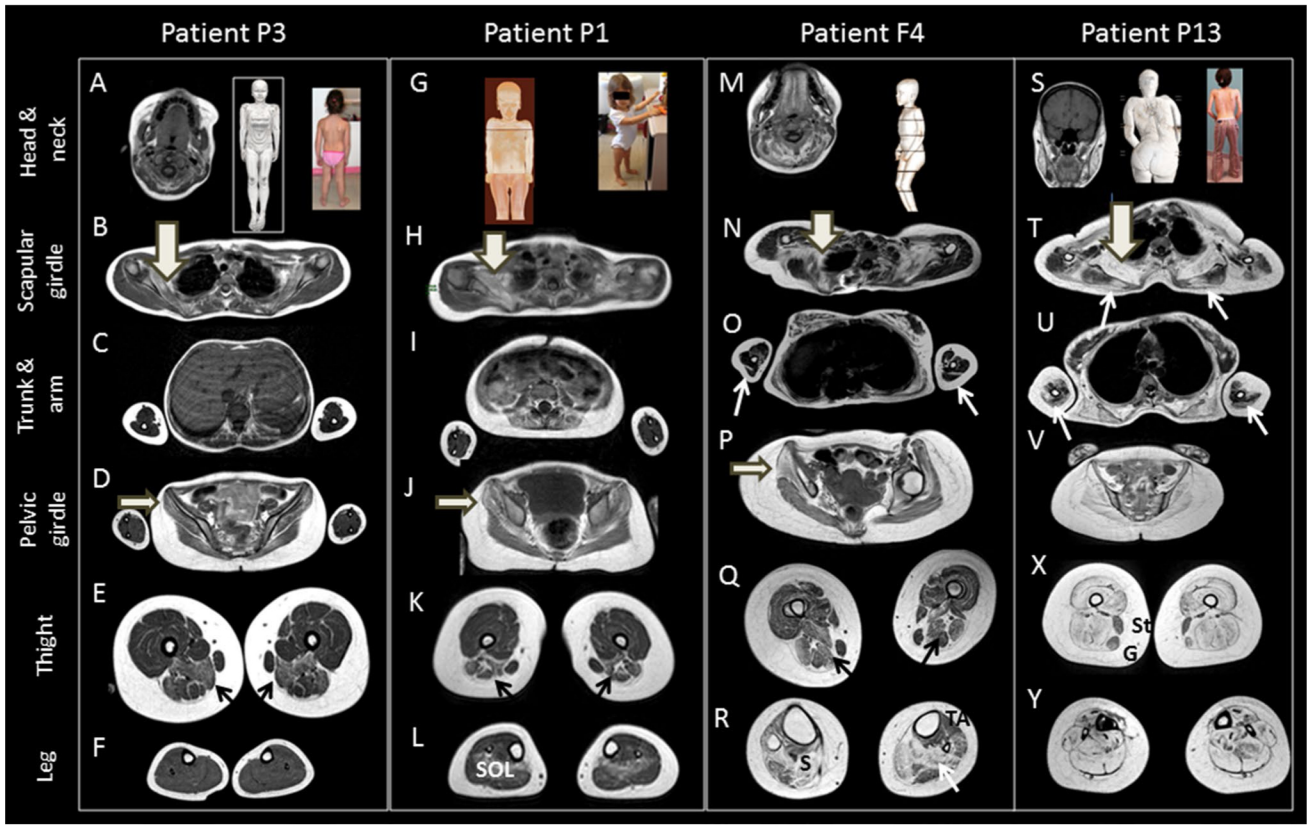

Fig. 4 WBMRI in LAMA2-RD using T1-weighted images (A–S; L–Y) and IDEAL T2 (only fat) Dixon techniques. It shows muscle images from three ambulant patients (first on the right and both on the left) and one non-ambulant boy with joint contractures (second on the right). Axial views of the cervico-cranial region are presented in two cases (A, M) and frontal views of the head are shown in one (S). No major involvement of masticator muscles or tongue is seen in ambulant patients but marked fatty replacement is observed in the neck extensors and tongue in the non-ambulant child (M). 3D reconstructions and clinical pictures are shown in the upper part of the figure for all four patients. Axial views at different levels of the body (shoulders, trunk and arms, pelvis and forearms, thighs and legs) show a homogeneous muscle pattern of involvement in the four patients with: **a** striking subscapular fatty replacement (thick vertical white arrows in B, H, N, T); **b** Gluteus medius and minimus abnormalities in the pelvis heatmaps (horizontal white thick arrows in D, J, P); **c** involvement of the posterior region of the thigh in particular adductor magnus and biceps femoris (black arrows in F, K, Q); **d** a "negative" pattern, characterized by diffuse and severe fat replacement in the thigh and sparing of sartorius (St) and gracilis muscles (G). In the leg, the Soleus (SOL) is the first muscle to be affected (R) and then the posterior and anterior leg become abnormal (Y). Note in particular in the oldest patients (two on the right) that there are multiple muscles showing "tigroid" aspect as it is seen in COL6 myopathies (thin white arrows at the triceps muscles (O, U), suprascapular (T) and soleus muscle(R). Note that the most severe abnormalities are not seen in the most severe patient (non-ambulant, second on the right) but in the oldest (first on the right)

spectrum of onset and severity. WBMRI signal abnormalities on T1-weighted sequences or fat-only Dixon images show a homogeneous fat replacement pattern (LAMA2-RD "fingerprint") with a continuum from MDC1A to LGMD-R23. The main regions of interest are not only the inferior limbs but also the shoulder and trunk (early involvement of subscapularis and serratus anterior muscles) and the pelvic girdle (preferential involvement of the gluteus medius and minimus). In the thigh, medial and posterior compartments are affected predominantly, overlapping with other inherited myopathies (adductor magnus, LHBF and hamstrings) [8, 30]. In the case of anterior thigh involvement, no differences are observed between rectus anterior and vastii muscles. At the axial level, thoracic region is better preserved than lumbar one. The set of affected muscles delineates a "positive" pattern in early and moderately advanced stages of the disease, but in later stages, the key muscles for diagnosis are not the most affected but rather those relatively preserved ("negative" fingerprint) such as levator scapulae, the forearm, the anterior leg muscles (tibialis anterior), and in the thigh, gracilis, sartorius and adductor longus muscles.

Remarkably, sequences used to study muscle inflammation or edema are also useful to identify white matter abnormalities in the brain, which is a definitive clue for diagnosis and highlights the interest of WBMRI protocols including head scanning with STIR or T2 fat sat Dixon sequences as a

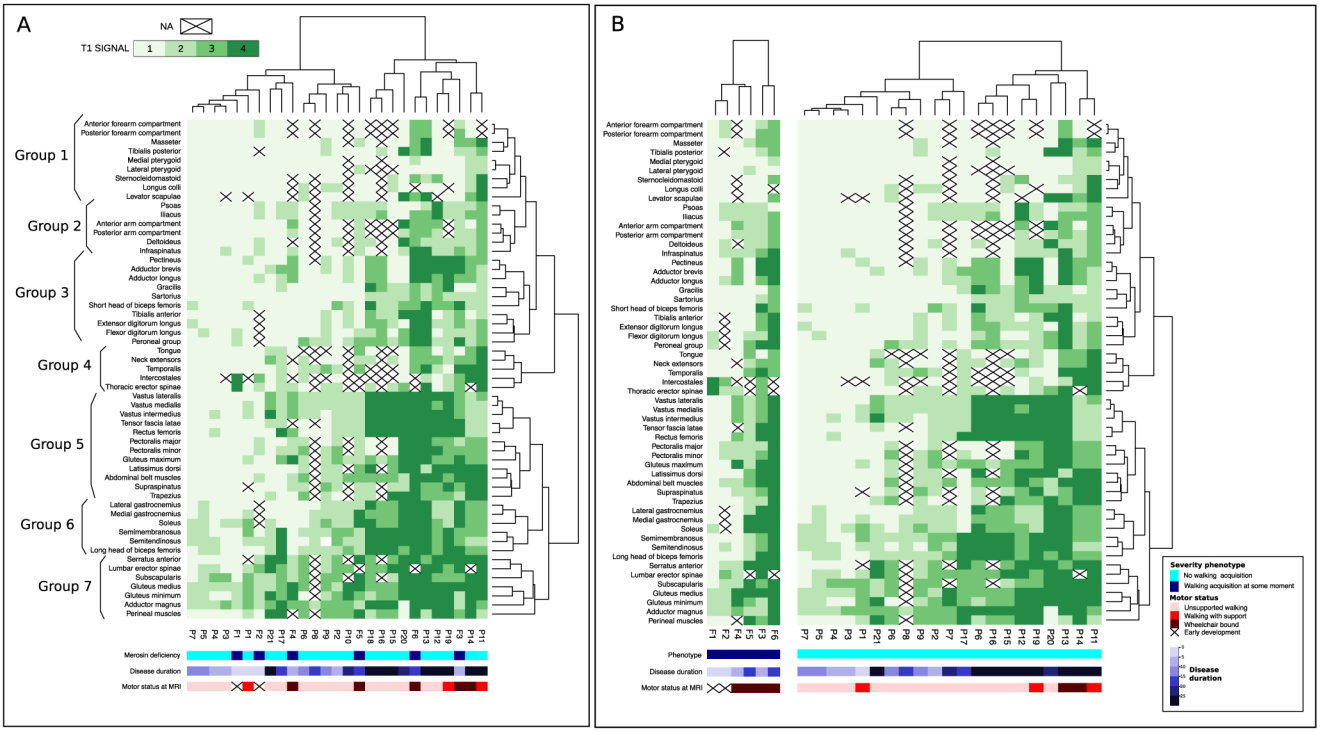

Fig. 5 Hierarchical heatmaps representing scores for T1 signal in ambulant and non-ambulant LAMA2-RD (**A** Whole cohort. **B** Ambulant—right—and non-ambulant patients—left—split into 2 separated parts). In these heatmaps, muscles are also ordered according to similarity in fat replacement. Notice the preservation of the patterns between these groups and the high dependence on disease duration

routine practice. White matter involvement was detectable by both techniques but subtle involvement (more typical in milder cases) was less visible on STIR. This has convinced us to recommend IDEAL T2 WBMRI examination (Dixon). We did not detect edema or inflammatory signs in muscle in the patients of our study, but this should be confirmed in larger series with young children and patients at earlier stages of the disease than ours, and using Dixon techniques rather than STIR.

Overall, this study shows that WBMRI can provide useful information to orientate diagnosis in LAMA2-RD patients, or to interpret conflicting genetic or biopsy findings. Immunolabeling of merosin is sometimes misleading with secondary merosin reduction in some muscle disorders and conversely, with positive immunolabeling of merosin if only one antibody is used, as it happened in two of the cases in our study [31]. Muscle imaging fingerprints are particularly interesting in the era of next-generation sequencing because they can further support or rule out molecular results, as cases of variants of unknown significance and in genes that can harbor intragenic duplications and deletions such as *LAMA2* [7, 22, 32]. Remarkably, in our cohort, some molecular diagnoses were supported by the imaging phenotype. For example, compatibility of WBMRI findings with the LAMA2-RD fingerprint supported the interpretation of the variant c.909 + 7A > G in intron 6 as pathogenic in four Chilean patients from three unrelated families. Also, a Danish ambulant adult carried a pathogenic variant at the heterozygous state and a second variant which was initially considered as pathogenic [3]. Updated LAMA2 gene databases revealed that it was a benign polymorphism and subsequent re-sequencing supported by phenotypic findings (including imaging) identified the pathogenic mutation. Differential diagnosis of LAMA2-RD is broad. In Table 2, we have summarized the main clinical and imaging differential diagnoses with those imaging signs that would be helpful in the WBMRI apart from detecting the typical brain white matter abnormalities [33, 34].

A recent, interesting study by other group assessed the pattern of fat replacement in a group of 7 patients with LAMA2-related congenital muscular dystrophy [39]. This smaller study provides with a narrative description of fat replacement in a lower number of muscles and it does not include the data analysis techniques we were able to incorporate in this larger cohort with wider inclusion criteria and using systematic scoring. There are some differences between the proposed patterns. For instance, we found that adductor magus is more and earlier involved than brevis. Calf muscles are not universally involved in our cases and relative sparing of semitendinosus is not always present in our series. We think that these different findings are attributable to differences between series, including size and

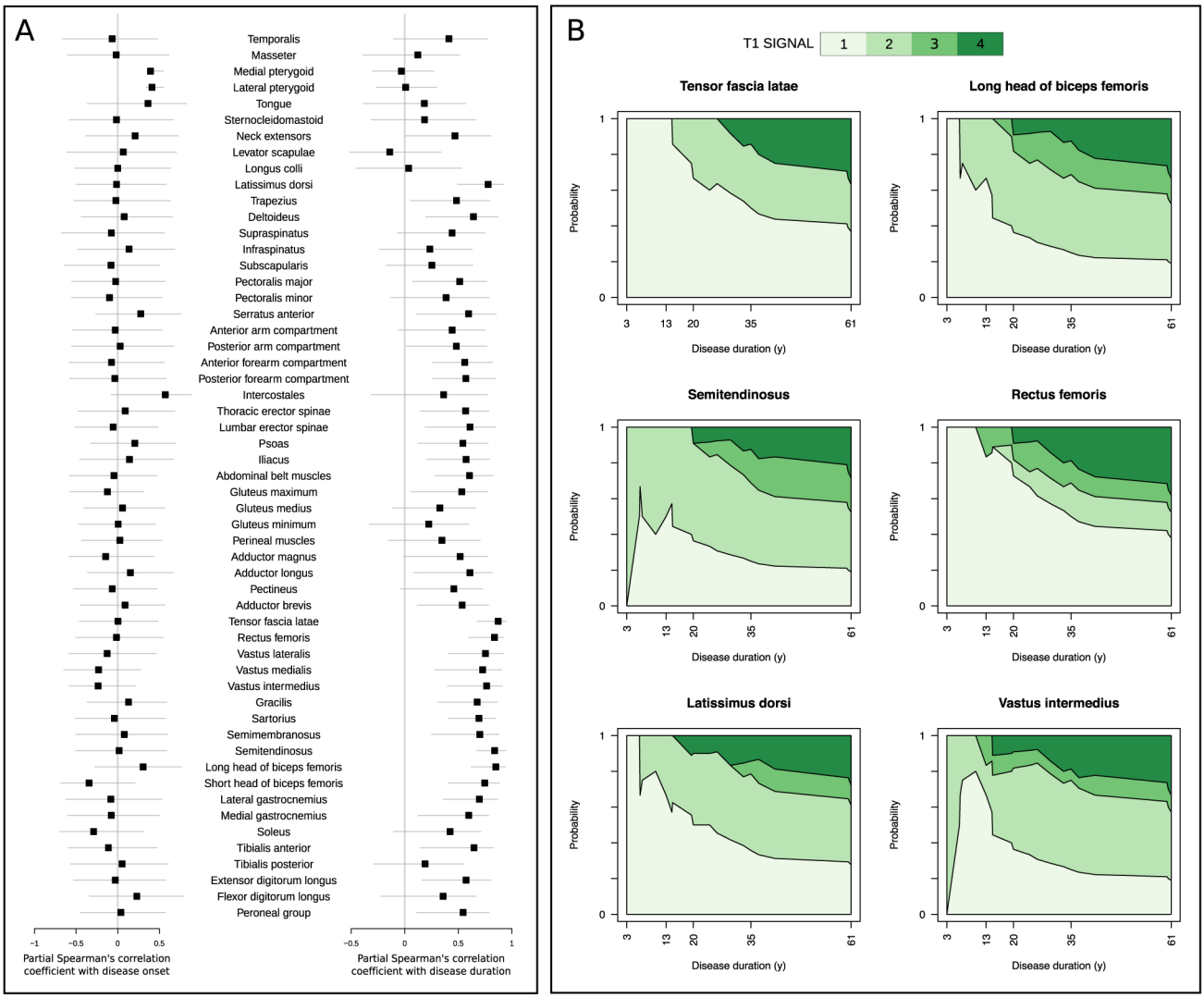

Fig. 6 **A** Forest plots showing the estimated partial Spearman's correlation and its 95% confidence interval of muscle replacement score for each muscle with disease onset (left) and with disease duration (right). Notice higher correlation for disease duration and higher coefficients for thigh muscles. **B** Estimation of cumulative probability of having a score of fatty replacement equal or below than 1, 2, 3 and 4 along disease duration in the 6 most correlated muscles

over all, inclusion criteria, and to different methods of data analysis.

An unexpected finding in this study was a significant discordance between muscle T1 signal and motor function. Several adult cases with preserved ambulation at the time of the examination showed diffuse intense signal abnormalities, while young children with a more severe phenotype had only slight changes. In fact, the degree of muscle T1 signal correlated with disease duration in ambulant patients, but not with a marker of disease severity as age at onset. This discordance is also found in other muscle diseases involving extracellular matrix such as collagenopathies, suggesting a similar physiopathology. Apposition of fibrotic tissue rather than a whole replacement of muscle fibers by fat would be a possible explanation [40, 41]. This type of findings suggests that the relationship between imaging biomarkers and potential disease mechanisms should be carefully analyzed in animal models and future studies in this group of disorders. Although no serial examinations were available and the quantification of the correlation in non-ambulant group was hampered by the limited sample size, our results suggest that adipose replacement seems to progress faster in non-ambulant patients. A larger sample with additional longitudinal data and functional tests is needed to understand the variations of the imaging phenotype throughout disease course within different severity degrees, but our study is already highlighting some

muscles in the thigh and pelvic region whose T1 signal scores would be more related to disease duration that should be targeted in future prospective imaging studies. An interesting issue regarding the distribution between muscles is that LAMA2-related muscle disorder has also a component of peripheral neuropathy. Although we do not have data from concomitant EMG studies and this limits our conclusions, distal involvement was specifically found in cases with an evolved disease that were the ones that are expected to show additional nerve involvement.

Our study also shows some interesting findings about genotype and genotype–phenotype correlation. Mutations are scattered all over the entire *LAMA2* coding region (Fig. 1) but predominantly in the first part of the protein (76%) with a few clustered at exon 13. In our cohort and in accordance to previous results [2, 7], non-ambulant patients harbored protein-truncating variants or splice-site mutations in both alleles. Patients who reached independent ambulation have at least one missense variant or in-frame deletions, preferentially distributed to the 5' regions, which may not lead to a dramatic reduction of laminin-α2 expression but affects its functioning [40]. While Oliveira et al. [7] described a limited number of variants in domain IVb and most of them were nonsense; in our series, they were relatively frequent and of different types. Another notable finding in our cohort is the description of two large exonic deletions (exons 9–34 and 23–34) in the same non-ambulant patient.

In conclusion, our work shows that WBMRI is a valuable diagnostic tool for muscle disorders due to LAMA2 mutations and could be useful in the follow-up, as it assesses both muscle and brain and detects muscle changes that evolve with the disease.

Table 2 Differential diagnosis of LAMA2-RD and relevant imaging signs for each disorder

Differential diagnosis	Phenotypic overlap	Shared imaging signs	Imaging signs that favors alternative diagnosis
LMNA-related muscular dystrophy[2, 8, 35]	EDMD-like phenotypes	Preferential involvement of gluteus medius and minimus in comparison to gluteus maximus Early involvement of adductor magnus	Predominant distal involvement of lower limbs Selective replacement of vastus lateralis
FKRP-related disorders[10, 36]	High CK levels Secondary reduction of merosin expression	Predominant involvement of adductor magnus	Early involvement of gluteus maximus, psoas, gastrocnemii and triceps Vastii progressive involvement and sparing of rectus femoris
Collagenopathies	Some LAMA2-RD may have a Bethlem-like phenotype [11]	"Sandwich-like" texture [8, 29]	Selective involvement of gluteus maximus compared to other glutei Absence of selective involvement of subscapularis
Juvenile Pompe disease [18]	EDMD-like phenotypes	Predominant involvement of subscapularis and adductor magnus	Striking involvement of the tongue Perservation of rectus femoris in comparison to vastii
Becker muscular dystrophy[37]	LGMD with high CK	Predominant involvement of adductor magnus	Early and predominant involvement of gluteus maximus
Calpainopathies [38]	LGMD with high CK	Predominant involvement of adductor magnus and relative preservation of gluteus maximus	Early involvement of adductor longus Marked featuring involvement of posterior thigh compartment Different involvement in the erector spinae muscles Systematic preservation of masseter and temporalis in advanced cases
Dysferlinopathies [27]	LGMD with high CK	Relative preservation of gracilis and sartorius	Relatively severe involvement of the distal lower limb muscles Systematic involvement of tibialis posterior and anterior forearm compartment in advanced cases

Acknowledgements We thank patients and families for their generous collaboration. We thank all MRI technical teams involved in the muscle imaging acquisition for their technical excellence and continuous support for performing neuromuscular imaging. This work is generated within the European Reference Network for Neuromuscular Diseases, FILNEMUS (French Neuromuscular Network) and the MYO-MRI COST-Action BM1304. We thank ISCIII for the financial support for studying LAMA2-RD in Spain.

Funding No direct funding supported this study. Indirect contributions are recognized in acknowledgement section.

Availability of data and material (data transparency) Complete data are shown in the manuscript or in supplementary material. Images are available for other researchers upon reasonable request.

Code availability (software application or custom code) R code is available upon reasonable request.

Declarations

Conflicts of interest The authors declare that they have no conflict of interest.

References

1. Allamand V, Guicheney P (2002) Merosin-deficient congenital muscular dystrophy, autosomal recessive (MDC1A, MIM#156225, LAMA2 gene coding for alpha2 chain of laminin). Eur J Hum Genet EJHG **10**(2):91–94: https://doi.org/10.1038/sj.ejhg.5200743
2. Geranmayeh F, Clement E, Feng LH et al (2010) Genotype-phenotype correlation in a large population of muscular dystrophy patients with LAMA2 mutations. Neuromuscul Disord NMD 20(4):241–250. https://doi.org/10.1016/j.nmd.2010.02.001
3. Lokken N, Born AP, Duno M et al (2015) LAMA2-related myopathy: Frequency among congenital and limb-girdle muscular dystrophies. Muscle Nerve 52(4):547–553. https://doi.org/10.1002/mus.24588
4. Gavassini BF, Carboni N, Nielsen JE et al (2011) Clinical and molecular characterization of limb-girdle muscular dystrophy due to LAMA2 mutations. Muscle Nerve 44(5):703–709. https://doi.org/10.1002/mus.22132
5. Marques J, Duarte ST, Costa S et al (2014) Atypical phenotype in two patients with LAMA2 mutations. Neuromuscul Disord NMD 24(5):419–424. https://doi.org/10.1016/j.nmd.2014.01.004
6. Sewry CA, D'Alessandro M, Wilson LA et al (1997) Expression of laminin chains in skin in merosin-deficient congenital muscular dystrophy. Neuropediatrics 28(4):217–222. https://doi.org/10.1055/s-2007-973703
7. Oliveira J, Gruber A, Cardoso M et al (2018) LAMA2 gene mutation update: Toward a more comprehensive picture of the laminin-alpha2 variome and its related phenotypes. Hum Mut 39(10):1314–1337. https://doi.org/10.1002/humu.23599
8. Quijano-Roy S, Avila-Smirnow D, Carlier RY et al (2012) Whole body muscle MRI protocol: pattern recognition in early onset NM disorders. Neuromuscul Disord NMD 22(Suppl 2):S68–S84. https://doi.org/10.1016/j.nmd.2012.08.003
9. Warman Chardon J, Diaz-Manera J, Tasca G et al (2019) MYO-MRI diagnostic protocols in genetic myopathies. Neuromuscul Disord NMD 29(11):827–841. https://doi.org/10.1016/j.nmd.2019.08.011
10. Tordjman M, Dabaj I, Laforet P et al (2018) Muscular MRI-based algorithm to differentiate inherited myopathies presenting with spinal rigidity. Eur Radiol 28(12):5293–5303. https://doi.org/10.1007/s00330-018-5472-5
11. Harris E, McEntagart M, Topf A et al (2017) Clinical and neuroimaging findings in two brothers with limb girdle muscular dystrophy due to LAMA2 mutations. Neuromuscul Disord NMD 27(2):170–174. https://doi.org/10.1016/j.nmd.2016.10.009
12. Nelson I, Stojkovic T, Allamand V et al (2015) Laminin alpha2 Deficiency-related muscular dystrophy mimicking Emery-Dreifuss and collagen VI related diseases. J Neuromuscul Dis 2(3):229–240. https://doi.org/10.3233/JND-150093
13. Mercuri E, Muntoni F (2012) The ever-expanding spectrum of congenital muscular dystrophies. Ann Neurol 72(1):9–17. https://doi.org/10.1002/ana.23548
14. Qiao C, Dai Y, Nikolova VD et al (2018) Amelioration of Muscle and Nerve Pathology in LAMA2 Muscular Dystrophy by AAV9-Mini-Agrin. Molecul Therapy Methods Clin Develop 9:47–56. https://doi.org/10.1016/j.omtm.2018.01.005
15. Gawlik KI, Durbeej M (2020) A Family of Laminin alpha2 Chain-Deficient Mouse Mutants: Advancing the Research on LAMA2-CMD. Front Molecul Neurosci 13:59. https://doi.org/10.3389/fnmol.2020.00059
16. Sarkozy A, Foley AR, Zambon AA et al (2020) LAMA2-related dystrophies: clinical phenotypes, disease biomarkers, and clinical trial readiness. Front Molecul Neurosci 13:123. https://doi.org/10.3389/fnmol.2020.00123
17. Richards S, Aziz N, Bale S et al (2015) Standards and guidelines for the interpretation of sequence variants: a joint consensus recommendation of the American College of Medical Genetics and Genomics and the Association for Molecular Pathology. Genet Med 17(5):405–424. https://doi.org/10.1038/gim.2015.30
18. Carlier RY, Laforet P, Wary C et al (2011) Whole-body muscle MRI in 20 patients suffering from late onset Pompe disease: Involvement patterns. Neuromuscul Disord NMD 21(11):791–799. https://doi.org/10.1016/j.nmd.2011.06.748
19. Quijano-Roy S, Carlier RY (2019) Neuroimaging in Non-dystrophic Myopathies. In: Barkhof F, Jager R, Thurnher M et al (eds) Clinical Neuroradiology: The ESNR Textbook. Springer International Publishing, Cham, pp 1–40
20. Lamminen AE (1990) Magnetic resonance imaging of primary skeletal muscle diseases: patterns of distribution and severity of involvement. British J Radiol 63(756):946–950. https://doi.org/10.1259/0007-1285-63-756-946
21. Hankiewicz K, Carlier RY, Lazaro L et al (2015) Whole-body muscle magnetic resonance imaging in SEPN1-related myopathy shows a homogeneous and recognizable pattern. Muscle Nerve 52(5):728–735. https://doi.org/10.1002/mus.24634
22. Ge L, Liu A, Gao K et al (2018) Deletion of exon 4 in LAMA2 is the most frequent mutation in Chinese patients with laminin alpha2-related muscular dystrophy. Scient Rep 8(1):14989. https://doi.org/10.1038/s41598-018-33098-3
23. Dello Russo C, Di Giacomo G, Mesoraca A et al (2014) Next generation sequencing in the identification of a rare genetic disease from preconceptional couple screening to preimplantation genetic diagnosis. J Prenatal Med 8(1–2):17–24
24. Savarese M, Di Fruscio G, Mutarelli M et al (2014) MotorPlex provides accurate variant detection across large muscle genes both in single myopathic patients and in pools of DNA samples.

Acta Neuropathologica Communic 2:100. https://doi.org/10.1186/s40478-014-0100-3
25. Stehlikova K, Skalova D, Zidkova J et al (2017) Muscular dystrophies and myopathies: the spectrum of mutated genes in the Czech Republic. Clin Genet 91(3):463–469. https://doi.org/10.1111/cge.12839
26. Zenagui R, Lacourt D, Pegeot H et al (2018) A reliable targeted next-generation sequencing strategy for diagnosis of myopathies and muscular dystrophies, especially for the giant titin and nebulin genes. J Molecul Diagnost JMD 20(4):533–549. https://doi.org/10.1016/j.jmoldx.2018.04.001
27. Gomez-Andres D, Diaz J, Munell F et al (2019) Disease duration and disability in dysfeRlinopathy can be described by muscle imaging using heatmaps and random forests. Muscle Nerve 59(4):436–444. https://doi.org/10.1002/mus.26403
28. Gomez-Andres D, Dabaj I, Mompoint D et al (2016) Pediatric laminopathies: Whole-body magnetic resonance imaging fingerprint and comparison with Sepn1 myopathy. Muscle Nerve 54(2):192–202. https://doi.org/10.1002/mus.25018
29. Mercuri E, Lampe A, Allsop J et al (2005) Muscle MRI in Ullrich congenital muscular dystrophy and Bethlem myopathy. Neuromuscul Disord NMD 15(4):303–330. https://doi.org/10.1016/j.nmd.2005.01.004
30. Tasca G, Monforte M, Diaz-Manera J et al (2018) MRI in sarcoglycanopathies: a large international cohort study. J Neurol Neurosurg Psychiatry 89(1):72–77. https://doi.org/10.1136/jnnp-2017-316736
31. Sewry CA, Naom I, D'Alessandro M et al (1997) Variable clinical phenotype in merosin-deficient congenital muscular dystrophy associated with differential immunolabelling of two fragments of the laminin alpha 2 chain. Neuromuscul Disord NMD 7(3):169–175. https://doi.org/10.1016/s0960-8966(97)00425-2
32. Oliveira J, Goncalves A, Oliveira ME et al (2014) Reviewing large LAMA2 deletions and duplications in congenital muscular dystrophy patients. J Neuromuscul Dis 1(2):169–179
33. Bonnemann CG, Wang CH, Quijano-Roy S et al (2014) Diagnostic approach to the congenital muscular dystrophies. Neuromuscul Disord NMD 24(4):289–311. https://doi.org/10.1016/j.nmd.2013.12.011
34. Leite CC, Lucato LT, Martin MGM et al (2005) Merosin-deficient congenital muscular dystrophy (CMD): a study of 25 Brazilian patients using MRI. Pediatr Radiol 35(6):572–579. https://doi.org/10.10007/s00247-004-1398-y
35. Diaz-Manera J, Alejaldre A, Gonzalez L et al (2016) Muscle imaging in muscle dystrophies produced by mutations in the EMD and LMNA genes. Neuromuscul Disord NMD 26(1):33–40. https://doi.org/10.1016/j.nmd.2015.10.001
36. Brockington M, Yuva Y, Prandini P et al (2001) Mutations in the fukutin-related protein gene (FKRP) identify limb girdle muscular dystrophy 2I as a milder allelic variant of congenital muscular dystrophy MDC1C. Hum Mol Genet 10(25):2851–2859. https://doi.org/10.1093/hmg/10.25
37. Barp A, Bello L, Caumo L et al (2017) Muscle MRI and functional outcome measures in Becker muscular dystrophy. Scient Rep 7(1):16060. https://doi.org/10.1038/s41598-017-16170-2
38. Barp A, Laforet P, Bello L et al (2020) European muscle MRI study in limb girdle muscular dystrophy type R1/2A (LGMDR1/LGMD2A). J Neurol 267(1):45–56. https://doi.org/10.1007/s00415-019-09539-y
39. Sakr HM, Fahmy N, Elsayed NS et al (2021) Whole-body muscle MRI characteristics of LAMA2-related congenital muscular dystrophy children: An emerging pattern. Neuromuscul Disord. https://doi.org/10.1016/j.nmd.2021.06.012
40. Gillies AR, Lieber RL (2011) Structure and function of the skeletal muscle extracellular matrix. Muscle Nerve 44(3):318–331. https://doi.org/10.1002/mus.22094
41. Yurchenco PD, McKee KK, Reinhard JR, et al. Laminin-deficient muscular dystrophy: Molecular pathogenesis and structural repair strategies. Matrix Biol 2018;71–72:174–187 https://doi.org/10.1016/j.matbio.2017.11.009

Authors and Affiliations

Susana Quijano-Roy[1,2] · Jana Haberlova[3] · Claudia Castiglioni[4,5] · John Vissing[6] · Francina Munell[7] · François Rivier[8,9] · Tanya Stojkovic[10] · Edoardo Malfatti[11] · Marta Gómez García de la Banda[1] · Giorgio Tasca[12] · Laura Costa Comellas[7] · Audrey Benezit[1] · Helge Amthor[1,2] · Ivana Dabaj[1,13] · Clara Gontijo Camelo[14] · Pascal Laforêt[15] · John Rendu[16] · Norma B. Romero[17,18] · Eliana Cavassa[1] · Fabiana Fattori[19] · Christophe Beroud[20] · Jana Zídková[21] · Nicolas Leboucq[22] · Nicoline Løkken[6] · Ángel Sanchez-Montañez[23] · Ximena Ortega[24] · Martin Kynčl[25] · Corinne Metay[26,27] · David Gómez-Andrés[7] · Robert Y. Carlier[28]

1 APHP, GH Université Paris-Saclay, Neuromuscular Center, Child Neurology and ICU Department, Raymond Poincare Hospital, Garches, France

2 Université de Versailles, U1179 INSERM-UVSQ, Versailles, France

3 Department of Paediatric Neurology, Motol University Hospital, Prague, Czech Republic

4 Pediatric Neurology Department, Clinica Las Condes, Santiago de Chile, Chile

5 Instituto Nacional de Rehabilitación Pedro Aguirre Cerda, Santiago de Chile, Chile

6 Department of Neurology, Rigshospitalet, University of Copenhagen, Copenhagen, Denmark

7 Pediatric Neurology, Vall d'Hebron Institut de Recerca (VHIR), Hospital Universitari Vall d'Hebron, Vall d'Hebron Barcelona Hospital Campus, Barcelona, Spain, Passeig de la Vall d'Hebron 119-129, 08035

8 Department of Pediatric Neurology and Reference Center for Neuromuscular Diseases AOC, CHU Montpellier, Montpellier, France

9 PhyMedExp, University of Montpellier, INSERM, CNRS, Montpellier, France

10 APHP, Neuromuscular Reference Center, Pitié-Salpêtrière Hospital, Institute of Myology, Paris, France

11 Univ Paris Est UPE, INSERM, U955 IMRB, APHP, Centre de Référence de Pathologie Neuromusculaire Nord-Est-Ile-de-France, Hôpital Henri Mondor, Créteil, France

[12] Unità Operativa Complessa Di Neurologia, Fondazione Policlinico Universitario A. Gemelli IRCCS, Roma, Italia

[13] CHU de Rouen, Service de Néonatologie, Réanimation pédiatrique, Neuropédiatrie et Éducation Fonctionnelle de L'enfant, INSERM U 1245, ED497, 76000 Rouen, France

[14] Department of Neurology, Faculdade de Medicina da Universidade de São Paulo (FMUSP), São Paulo, Brazil

[15] Nord/Est/Ile de France Neuromuscular Reference Center, PHENIX FHU, Hôpital Raymond-Poincaré, AP-HP. INSERM U1179, Garches, France

[16] Univ. Grenoble Alpes, Inserm, U1216, CHU Grenoble Alpes, GIN, Grenoble, France

[17] Sorbonne Université, Myology Institute, Neuromuscular Morphology Unit, Center for Research in Myology, GH Pitié-Salpêtrière, Paris, France

[18] Centre de Référence de Pathologie Neuromusculaire Paris-Est, GHU Pitié-Salpêtrière, Assistance Publique-Hôpitaux de Paris, Paris, France

[19] Unit for Neuromuscular and Neurodegenerative Disorders, Bambino Gesù Children's Hospital, Rome, Italy

[20] APHM, Laboratoire de Génétique Moléculaire, Hôpital TIMONE Enfants; Aix Marseille University, INSERM, MMG, Marseille, France

[21] Centre of Molecular Biology and Genetics, University Hospital Brno, Brno, Czech Republic

[22] Radiology Department, CHU Montpellier, Montpellier, France

[23] Pediatric Neuroradiology, Radiology Department, Hospital Universitari Vall d'Hebron, Vall d'Hebron Barcelona Hospital Campus, Barcelona, Spain

[24] Diagnostic Imaging Service, Clinica Las Condes, Santiago de Chile, Chile

[25] Department of Radiology, Motol University Hospital, Prague, Czech Republic

[26] AP-HP, UF Cardiogénétique et Myogénétique Moléculaire et Cellulaire, Centre de Génétique Moléculaire et Chromosomique, GH Pitié Salpêtrière, Paris, France

[27] Sorbonne Université - Inserm UMRS974, Centre de Recherche en Myologie, GH Pitié-Salpêtrière, Paris, France

[28] APHP, GH Université Paris-Saclay, DMU Smart Imaging, Medical Imaging Department, Raymond Poincaré Teaching Hospital, Garches, France